Geophys. J. R. astr. Soc. (1970) **21**, 285–294.

Computation of the Divergence Coefficient for Seismic Phases

Michael Shimshoni and Ari Ben-Menahem

(Received 1969 December 29)

Summary

By using a cubic spline interpolation method a representation of seismological travel-time tables is achieved which is highly continuous. Divergence coefficients for seismic phases computed from this representation are free from non-essential discontinuities and are thus more meaningful than those obtained using other methods of interpolation. Results are compared with those obtained by others. For six phases results are given in graphs and tables.

Recently the use of amplitudes in seismic studies has increased. Theoretical amplitudes can be obtained from travel times or from the structure of the Earth. If we had an 'exact' structure we could derive the amplitude distance relationship directly from it, but nothing would really be lost if we first computed a travel-time table and used it to obtain the amplitudes. In reality no exact structure is known, so if we have a good travel-time table it may serve as the source for an amplitude table. The present work deals with one aspect of obtaining theoretical amplitude tables for the various body-wave phases.

The amplitude is the result of various factors, among them geometric spreading, inelastic attenuation, the radiation pattern, etc. In addition, for phases which are reflected at boundaries (e.g., *PcP*, *PS*), the reflection factor is also to be considered. We are dealing with all these factors in a more general work; here we only want to report on a technique we use for obtaining the divergence coefficient caused by geometric spreading.

The divergence coefficient f can be obtained from the travel times (Singh & Ben-Menahem 1969) by

$$f^2 = \left| \frac{\rho_h v_h}{\rho_0 v_0} \frac{\sin i_h}{\sin\theta \cos i_0} \frac{di_h}{d\theta} \right|, \tag{1}$$

where the angles are as shown in Fig. 1. The suffix h always describes the focus and the suffix 0 indicates the level of the recording station (with or without stripping of the crust). v is the velocity of propagation of the wave and ρ is the density. We can recast this function into a more useful form in which parameters depending directly on the travel times appear as:

$$f^2 = \left| \frac{1}{r_0^3} \frac{\eta_0^2}{\rho_0} \cdot \frac{\rho_h}{\eta_h^2} r_h \cdot \frac{1}{\sin\theta} \cdot \frac{p\partial^2 t}{\partial\theta^2} \cdot \frac{1}{\sqrt{(\eta_0^2 - p^2)}} \cdot \frac{1}{\sqrt{(\eta_h^2 - p^2)}} \right|, \tag{2}$$

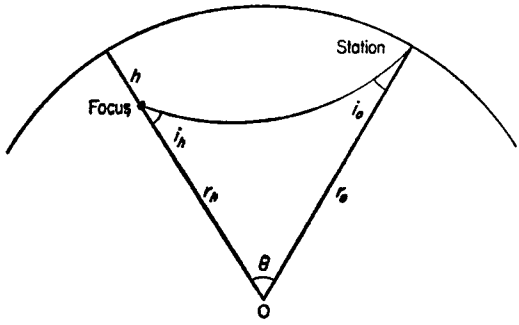

FIG. 1. Definitions for Formulae 1 and 2.

where r is the distance from the centre, $p = dt/d\theta$ is the ray parameter, $\eta = r/v$, and t is the travel time.

This last form of f underlines the difficulty of obtaining f from travel-time tables, as it depends not only on the first derivative of t with respect to θ, but on the second derivative as well. Thus using travel-time data as our input necessitates two numerical differentiations with all the problems that ensue.

One of the more recent works which include the computation of amplitudes is that of Julian & Anderson (1968). There, the starting point is from a known point structure of the Earth and Julian & Anderson derive the amplitudes resulting from this structure. If the Earth had full spherical symmetry, and if all its parameters were exactly known, amplitude factors of any desired accuracy could be obtained. In reality, as there is no such symmetry, and the parameters are only known up to certain error (in the best case), we deal only with an approximation, and we have to realize that our results are only approximately correct.

As an example we take the results of Julian & Anderson for Jeffreys's model. Jeffreys (1959) gives his velocities as a function of the relative radius r/R (R being the radius of the Earth up to the Moho 6338 km) for 1·00 (0·01) 0·90 and 0·90 (0·02) 0·56 and also for 0·55, after which the core, which is of no interest in our present work, is reached. Julian & Anderson computed the velocities for the region $r/R = 0{\cdot}94$ to $r/R = 0{\cdot}84$ using four-point Lagrangian interpolation, at steps of 0·005. For the actual computation of the amplitude factor and the other derived quantities a Mohorovičić velocity dependence of $v = ar^b$ between the points of distance $r/R = 0{\cdot}005$ is taken. This form of exponential interpolation is really very close to a linear one. By this procedure we get discontinuous variations of v not only at every tabulated point of Jeffreys, where the cubic interpolation function changes, but also to some degree at every derived point, as the almost linear interpolation function changes there. These discontinuous variations are important in the computation of amplitude factors, which are dependent on the first two derivatives of t, and these derivatives become discontinuous. In Fig. 2 we show Julian & Anderson's result, and attention is drawn to the region beyond the 20° discontinuity. It seems clear that the ' hooks ' seen in the amplitude curves are a result of the method of interpolation, and one cannot claim that they are an intrinsic property of Jeffreys's structure. If the cubic interpolation formula had been used to obtain more intermediate points, we would have a greater number of very small hooks, and only be left with bigger ones at points corresponding to Jeffreys's original tabulated velocities. As we cannot assume that the real Earth puts its discontinuities just at the points in Jeffreys's table, we are justified in saying that the hooks are a result of the computational method. We do not claim that there are no discontinuities; all we state is that we cannot find them from the data.

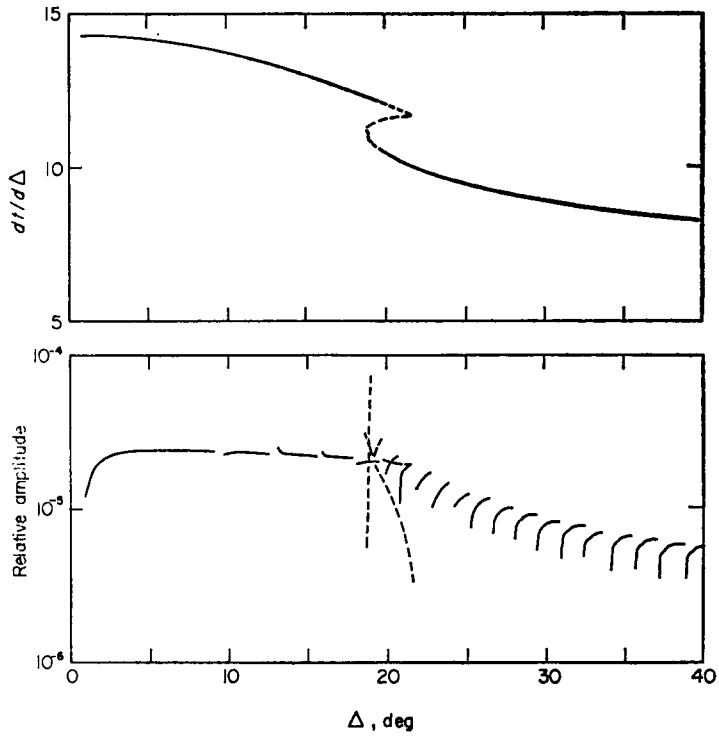

FIG. 2. Results of Julian and Anderson for '$dt/d\Delta$ and amplitude, considering geometric spreading only, for P waves in Jeffreys Earth Model Surface Focus'.

Our method uses as data the Jeffreys–Bullen travel times (1967) for surface foci, and we thus have a discrete set of information. As we need the first two derivatives of the times we have to use some form of interpolation (explicit or implicit). Lagrangian interpolation, or divided differences (which is another name for the same method), fits polynomials between two neighbouring points, causing discontinuities in the derivatives at every tabulated point. As an alternative we suggest the use of cubic splines as a method of interpolation. Curtis & Shimshoni (1970) have previously used cubic splines successfully in the somewhat related problem of smoothing observational seismic travel times.

Cubic splines get their name from a tool used by draftsmen to draw a continuous curve between points, using a flexible thin strip of wood (the spline). With this tool the draftsmen have a flexible French curve. The strip is anchored in place by weights, and made to pass through or near specified points. The resulting line has continuous curvature, with jumps in the rate of change of the curvature at the points of the weights (the joints or the knots). Mathematically the line is continuous and also has continuous first and second derivatives. At the joints, jumps of the third derivative are permitted, but between them the line is described by a cubic polynomial. Because of the continuity requirements, a curve with n joints is determined by just $n+2$ parameters.

The computational program finds the required number and location of the joints. Then we minimize the squares of the deviations at the original tabulated points, while attempting to minimize the jumps of the third derivatives at the joints. We try to use the smallest possible number of joints while still keeping the deviations

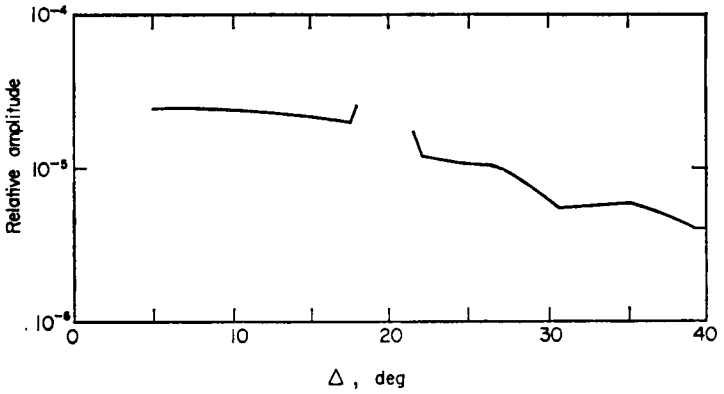

FIG. 3. Our results for the Julian and Anderson case.

within the uncertainties of the table. We also pay attention to the sign of the deviations; if we see that between two joints all the deviations or almost all of them have the same sign, we add another joint in the middle.

We used cubic splines on the surface foci table of Jeffreys & Bullen for P, and then computed the amplitude factor from the resulting travel-time function. Fig. 3 shows our amplitude factor which is also drawn on a logarithmic scale. Fig. 4 shows our result superimposed on that of Julian & Anderson. As the travel time of P is made up of two branches, one up to about 19° and the other from there onwards, we have a discontinuous first derivative near 19°. We thus fitted the table up to 19° by one cubic spline and the table from there to the end by another cubic spline. Formulae (1) and (2) are invalid at the discontinuity. We claim that our result is as good an approximation to the amplitude factor as can be obtained from the data.

In general, for phases with discontinuous derivatives, one can still use cubic splines as long as one remains on a single branch, and treats the other branches separately.

At the final stage, while computing the cubic spline values for the times of the P and S phases (surface foci), we thus split the range of interest into the two branches caused by the 20° discontinuity of the Jeffreys–Bullen times. We found that the two branches meet at a distance of about 19·6° for P and at a distance of about 20·3°

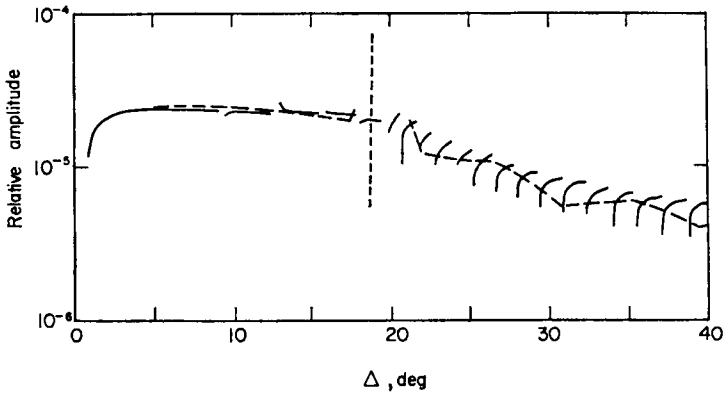

FIG. 4. Our results superimposed on those of Julian and Anderson.

Table 1

Divergence factors for P and S waves for deep focus ($h = 0{\cdot}06R$) events; the recording station is on the top of the mantle.

Δ	Divergence coefficients *P*	*S*	Δ	Divergence coefficients *P*	*S*
15	65·23	91·74	55	14·29	12·21
16	60·18	82·06	56	13·91	12·32
17	55·63	73·12	57	13·53	12·41
18	51·53	64·86	58	13·17	12·24
19	47·73	57·08	59	12·82	12·03
20	44·18	49·50	60	12·48	11·82
21	40·91	41·69	61	12·26	11·63
22	38·00	36·69	62	12·07	11·46
23	34·69	33·08	63	11·88	11·34
24	31·40	29·45	64	11·71	11·23
25	28·14	25·75	65	11·53	11·11
26	25·28	21·84	66	11·36	11·00
27	22·78	19·75	67	11·21	11·05
28	20·26	17·74	68	11·08	11·10
29	18·87	15·67	69	10·95	11·13
30	19·87	13·47	70	10·82	11·17
31	20·68	13·20	71	10·69	11·00
32	20·97	14·67	72	10·57	10·67
33	19·07	15·86	73	10·44	10·36
34	17·13	16·84	74	10·30	10·04
35	15·12	17·58	75	10·16	9·78
36	14·46	17·29	76	10·03	9·85
37	13·84	17·01	77	9·90	9·90
38	13·25	16·74	78	9·77	9·95
39	14·35	16·48	79	9·64	10·00
40	15·50	16·08	80	9·50	10·04
41	16·45	15·59	81	9·37	10·08
42	16·43	15·12	82	9·23	10·11
43	16·08	14·67	83	9·10	10·13
44	15·75	14·24	84	8·97	10·12
45	15·44	13·86	85	8·85	10·04
46	15·13	13·49	86	8·38	9·95
47	14·84	13·14	87	7·76	9·86
48	14·69	12·80	88	7·12	9·78
49	14·72	12·56	89	6·44	9·23
50	14·74	12·38	90	5·70	8·56
51	14·75	12·20	91	4·86	7·86
52	14·75	12·03	92	4·27	7·12
53	14·74	11·95	93	3·93	6·40
54	14·70	12·09	94	3·57	5·71
			95	3·16	4·94
			96	2·70	4·03
			97	2·15	2·95

Table 2

Divergence factors for PcP and ScS waves for deep focus ($h = 0{\cdot}06R$) events; the recording station is on the top of the mantle.

Δ	Divergence coefficients *PcP*	*ScS*	Δ	Divergence coefficients *PcP*	*ScS*
0	10·13	10·48	50	6·17	6·61
1	10·18	10·55	51	6·11	6·51
2	10·24	10·61	52	6·05	6·41
3	10·29	10·67	53	5·99	6·31
4	10·35	10·77	54	5·93	6·20
5	10·41	10·87	55	5·87	6·10
6	10·47	10·98	56	5·81	5·99
7	10·53	10·87	57	5·75	5·88
8	10·60	10·72	58	5·65	5·78
9	10·55	10·55	59	5·54	5·66
10	10·48	10·38	60	5·42	5·55
11	10·41	10·19	61	5·31	5·44
12	10·32	10·00	62	5·19	5·34
13	10·24	9·95	63	5·07	5·24
14	10·15	9·93	64	4·95	5·15
15	10·06	9·92	65	4·82	5·05
16	9·97	9·91	66	4·64	4·95
17	9·75	9·91	67	4·42	4·85
18	9·48	9·91	68	4·19	4·75
19	9·21	9·86	69	3·95	4·64
20	8·92	9·78	70	3·70	4·53
21	8·92	9·70	71	3·42	4·43
22	9·05	9·61	72	3·13	4·31
23	9·17	9·53	73	2·80	4·20
24	9·31	9·45	74	2·57	4·08
25	9·30	9·38	75	2·61	3·94
26	9·23	9·31	76	2·65	3·79
27	9·15	9·25	77	2·70	3·64
28	9·07	9·18	78	2·74	3·48
29	8·98	9·12	79	2·78	3·32
30	8·88	9·06	80	2·82	3·15
31	8·78	8·91	81	2·86	2·96
32	8·69	8·71	82	2·90	2·77
33	8·57	8·49	83	2·88	2·56
34	8·44	8·27	84	2·86	2·34
35	8·30	8·05	85	2·85	2·09
36	8·16	7·81	86	2·83	1·80
37	8·02	7·66	87	2·81	1·77
38	7·88	7·62	88	2·79	1·76
39	7·73	7·58	89	2·77	1·74
40	7·58	7·54	90	2·76	1·73
41	7·43	7·50	91	2·66	1·71
42	7·29	7·46	92	2·54	1·70
43	7·14	7·40	93	2·40	1·68
44	7·00	7·29	94	2·26	1·67
45	6·85	7·18	95	2·10	1·65
46	6·70	7·06	96	1·93	1·64
47	6·54	6·95	97	1·75	1·63
48	6·38	6·83			
49	6·23	6·71			

for S. At these points the travel times are still continuous, but the first derivatives are discontinuous. Because of this discontinuity, special care has to be taken when dealing with P and S times.

For P and S we also computed the splines for each depth given in the J–B Tables, starting with the distance 0° (where $dt/d\Delta = 0$) and reaching up to the distance where the ray leaves the focus horizontally; at the final distance $dt/d\Delta$ reaches its maximal value which equals $\eta = r/v$ for that depth.

We also computed splines for surface times of many other phases, and obtained their times and derivatives for deep focus events by the use of the P or S depth splines.

As an example, let us consider the phase PcS, the surface times of which equal those of ScP. After obtaining the surface times splines of PcS, we can match $dt/d\Delta$ of PcS algebraically with $dt/d\Delta$ of P times for a depth of, say, $h = 0{\cdot}06R$ (using the

Table 3

Divergence factors for PcS and ScP waves for deep focus ($h = 0{\cdot}06R$) events; the recording station is on the top of the mantle.

Δ	Divergence coefficients *PcS*	*ScP*	Δ	Divergence coefficients *PcS*	*ScP*
0	17·82	5·39	30	13·85	4·24
1	17·95	5·43	31	13·50	4·14
2	18·08	5·47	32	13·15	4·03
3	18·22	5·51	33	12·79	3·92
4	18·35	5·55	34	12·43	3·82
5	18·49	5·59	35	12·05	3·70
6	18·47	5·59	36	11·75	3·59
7	18·42	5·57	37	11·58	3·53
8	18·36	5·55	38	11·41	3·48
9	18·29	5·53	39	11·24	3·43
10	18·22	5·51	40	11·08	3·38
11	17·93	5·44	41	10·88	3·33
12	17·60	5·35	42	10·54	3·25
13	17·26	5·25	43	10·19	3·14
14	16·89	5·14	44	9·72	3·04
15	16·52	5·03	45	9·16	2·87
16	16·41	4·97	46	8·56	2·70
17	16·36	4·96	47	7·69	2·49
18	16·32	4·94	48	6·71	2·22
19	16·29	4·93	49	5·96	1·91
20	16·27	4·93	50	5·62	1·77
21	16·14	4·90	51	5·27	1·67
22	15·96	4·85	52	5·42	1·60
23	15·77	4·79	53	5·66	1·67
24	15·59	4·74	54	5·84	1·74
25	15·41	4·68	55	5·80	1·77
26	15·14	4·62	56	5·77	1·76
27	14·83	4·53	57	5·57	1·75
28	14·51	4·43	58	5·24	1·65
29	14·18	4·34	59	4·90	1·55
			60	4·41	1·44
			61	3·85	1·28

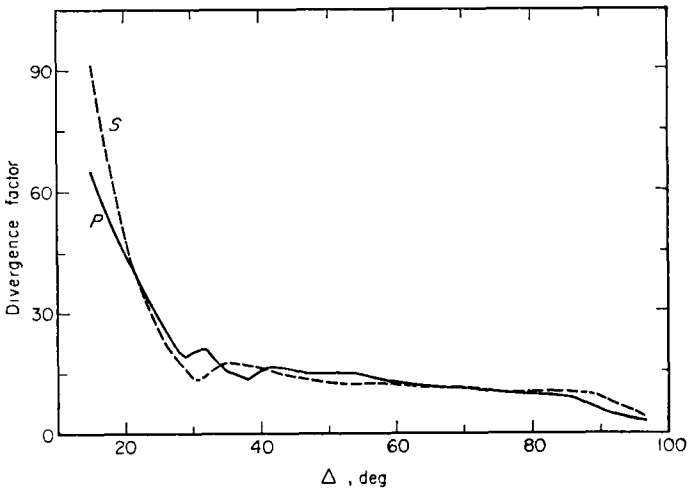

FIG. 5. Divergence factors for P and S waves for deep focus ($h = 0{\cdot}06R$) events; the recording station is on the top of the mantle.

notation of the J–B Tables). Let $dt/d\Delta$ of PcS (surface) at a distance Δ_1 equal $dt/d\Delta$ of P ($h = 0{\cdot}06R$) at Δ_2, and let t_1 be the time of PcS (surface) at Δ_1, and t_2 the time of P ($h = 0{\cdot}06R$) at Δ_2. From this it follows that at a distance $\Delta = \Delta_1 - \Delta_2$ the time of PcS ($h = 0{\cdot}06R$) equals $t_1 - t_2$. Moreover, at a distance $\Delta = \Delta_1 + \Delta_2$ the time of $pPcS$ ($h = 0{\cdot}06R$) equals $t_1 + t_2$. Since in each range the times are expressed as cubic polynomials, the problem of finding Δ_1 and Δ_2 for a given Δ reduces to the solution of a quadratic equation. With equal ease $dt/d\Delta$ and $d^2t/d\Delta^2$ at Δ are obtained for PcS ($h = 0{\cdot}06R$).

Thus we have all we need for using equation (2) and obtaining the divergence coefficients for various phases.

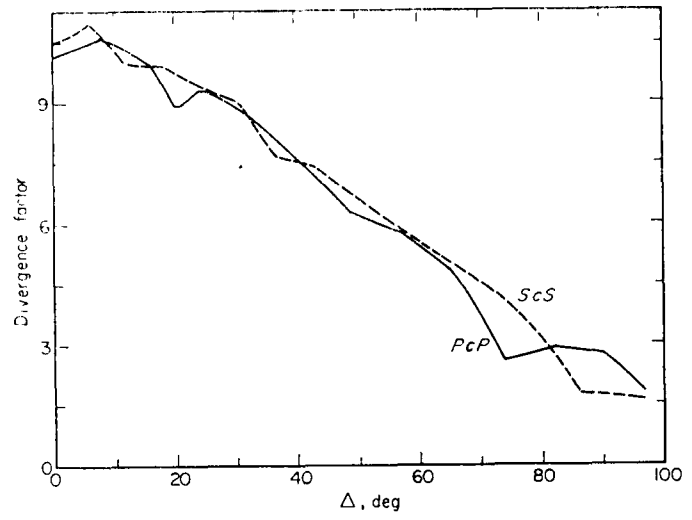

FIG. 6. Divergence factors for PcP and ScS waves for deep focus ($h = 0{\cdot}06R$) events; the recording station is on the top of the mantle.

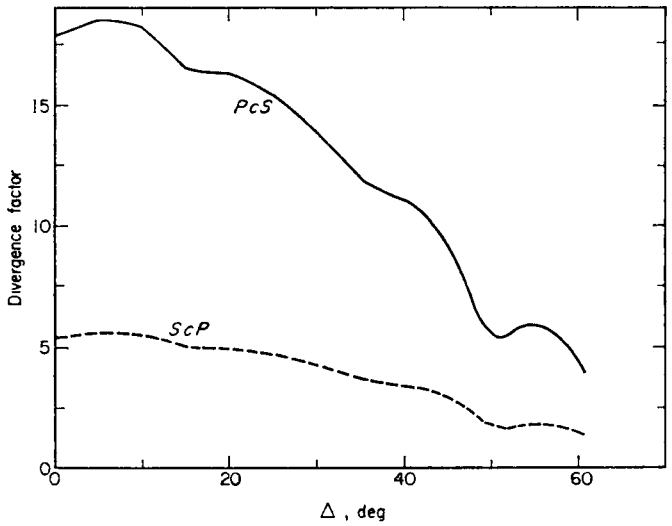

FIG. 7. Divergence factors for *PcS* and *ScP* waves for deep focus ($h = 0{\cdot}06R$) events; the recording station is on the top of the mantle.

As examples of our results we tabulate and plot the divergence factors of six phases for a depth of focus of $h = 0{\cdot}06R$ (about 400 km), and for a receiving station situated on the top of the Mantle (stripping away the crust).

In Tables 1–3 we give results for the phases *P*, *S*, *PcP*, *ScS*, *PcS* and *ScP*. In Figs 5–7 we display these coefficients graphically. The units of the divergence coefficients are not given, as only their relative values are of interest.

We left out distances near the end of the range if values of $dt/d\Delta$ and $d^2t/d\Delta^2$ were unreliable, because they were tied to the tables from one side only.

As stated earlier, no high claim for accuracy is made; an uncertainty of about 5 per cent can be expected. But it is claimed that our results give a clear idea of the values of the divergence coefficient which follow from the Jeffreys–Bullen times. Coefficients with smaller uncertainties are unobtainable, not only because of our limited knowledge of the structure of the Earth, but also because the deviations in this structure from spherical symmetry make higher accuracy meaningless.

Acknowledgment

This research has been supported by the U.S. Naval Office of Naval Research under Contract N00014–67–C0146 and by the Air Force Cambridge Research Laboratories under Contract AF61(052)–954 through the European Office of Aerospace Research, OAR, USAF, as part of the Advanced Research Projects Agency's Project Vela-Uniform.

Department of Applied Mathematics,
Weizmann Institute of Science,
Rehovot,
Israel.

References

Curtis, A. R. & Shimshoni, M., 1970. The smoothing of seismological travel-time tables using cubic splines. Submitted to *Bull. seism. Soc. Am.*

Jeffreys, H., 1959. *The Earth*, 4th Edition, Cambridge University Press.

Jeffreys, H. & Bullen, K. E., 1967. *Seismological Tables*, British Assoc. for the Advancement of Science, Gray Milne Trust, Burlington House, London, W.1.

Julian, B. R. & Anderson, D. L., 1968. Travel times, apparent velocities and amplitudes of body waves, *Bull. seism. Soc. Am.*, **58**, 339–366.

Singh, S. J. & Ben-Menahem, A., 1969. Asymptotic theory of body waves in a radially heterogeneous Earth, *Bull. seism. Soc. Am.*, **59**, 2039–2059.